Egyptian Journal of Chemistry

http://ejchem.journals.ekb.eg/

New Fe₂O₃ Nanoparticles Modified Carbon Paste Electrode: A Cyclic Voltametric Study

Emad Salaam Abood[1], Ahmed Salim Abed[1,] Zahraa Njah Salman[1]
[1]Department of Medical Physics, Hilla University College, Babylon, Iraq.

Abstract

The cyclic voltammetry (CV) technique was accustomed to look into the electro oxidation of iron ions in water using a novel carbon paste electrode CPE enhanced with iron oxide nanoparticles. The revised electrode exhibited a high resolving function, allowing the overlapping voltametric response of Fe-ion to be resolved into a single well-defined peak. The voltage differential between Epa (anodic) and Epc (cathodic) was higher than 200 mV; this range is referred to as the quest-reversible mechanism. At temperatures ranging from 15 to 35 °C, the kinetics of the electrode were investigated. Voltammogram data revealed a rise in temperature, which resulted in an increase in negative shift, diffusion electron transfer in the Fe redox reaction. The Randles-Sevcik equation yielded a diffusion coefficient of 4.9×10^{-5}; the rate constant K was 2.3×10^{-4}; and the peak current of Fe-ion rose linearly with concentrations ranging from 1 to 5 ppm**.
Keywords: Cyclic voltammetry; Electrode; Fe₂O₃ nanoparticles; Hydrothermal method.

Introduction

Metal nanoparticles, nano-diamonds, fullerenes, carbon nanotubes, and other nano-materials are being employed in biomedical and sensing applications because they have basic qualities such as reduced size, excellent optical, magnetic, and mechanical capabilities [1]. Due to their unique characteristics and a significant surface/volume ratio versus their bulk counterparts, metal nanoparticles have received far greater attention in recent decades [2]. For the determination of pharmaceuticals, many electrochemical techniques are available, and they have been described in the literature. The addition of various metal nanoparticles to carbon paste electrodes can increase sensitivity and selectivity, as a result, electron transfer between the electroactive species and the electrode surface occurs at a higher pace. Metal oxide nanoparticles MnO2 [3], NiO [4], CuO [5], and ZnO [6] as well as platinum [7], gold [8], silver [9], copper [10], and metal oxide nanoparticles [10] that have been utilized in the creation of electrochemical sensors have been described in the literature.[11] The Fe₂O₃ nanoparticles exhibited just a few distinct characteristics from massiveness phases. Fe2O nanoparticles' electronic, magnetic, and optical properties have a large number of possible uses in industry, includes novel electrical and optical devices, data storage, magnetocaloric cooling, color imaging,

bioprocessing, ferrofluid technologies, and magnetic recording media manufacturing [12].

Magnetite (Fe₃O₄) and its oxidized cousin maghemite are the two main kinds of iron oxide nanoparticles (Fe₃O₂). Their scarcity, inherent superparamagnetic characteristics, and prospective uses in a variety of sectors have sparked attention [13]. Iron oxide nanoparticles are used in a variety of applications, including terabit magnetic storage devices, catalysis, sensors, superparamagnetic relaxometry, high-sensitivity biomolecular magnetic resonance imaging, magnetic particle imaging, magnetic fluid hyperthermia, separation of biomolecules, and targeted drug and gene delivery for medical diagnosis and therapeutics [14-17]. Long-chain fatty acids, alkyl-substituted amines, and diols have been used to coat nanoparticles in these applications [17, 18]. [19] They've been used in supplement formulations. Co-precipitation of ferrous/ferric salts [20-22], thermal breakdown of hydrazine iron (II) oxalate [23], microemulsion [24], and sol-gel syntheses [25], hydrolysis, and pyrosis [26] have all been used to generate magnetite and maghemite. Coprecipitation affects nanoparticle size and form by varying iron salt production, as well as concentrations, surfactants, pH, and temperature [27, 28]. By calcining magnetite in the air, it becomes maghemite $4Fe_3O_4 + O_2 = 4Fe_3O_4 + O_2$. Maghemite possesses cationic vacancies in one-

_____

third of the octahedral sites, whereas magnetite has Fe^{3+} in all tetrahedral sites and Fe^{3+} and Fe^{2+} in octahedral sites. Because the magnetic characteristics of converted maghemite, such as remnant magnetization and saturation magnetization, and coercivity, are impacted by their preparation, their magnetic properties, Saturation magnetization, remanent magnetization, and coercivity, for example, may all be changed [29]. Magnetite, maghemite, and hematite have super paramagnetic characteristics [30]. In the air, super paramagnetic nanoparticles with high saturation magnetization may be produced [31]. In general, iron oxides are abundant, frequently employed despite their low cost, and play an important role in a variety of biological and geological processes. According to above survey, we aim to prepare new Fe_2O_3 nanoparticles modified carbon paste electrode via potentiodynamic electrochemical measurement (a cyclic Voltametric Study)

Excremental:

Preparation of Iron oxide nanoparticle by Hydro-thermal method.

The high surface area of iron oxide NPs suggests increased reactivity [32]. The iron (II) chloride tetrahydrate powder was dissolved in 10 mL distilled water, and 35 mL iso-butanol was added. After heating the aqueous-organic combination to 75°C, 0.5 M NaOH was added dropwise for 4 hours while stirring continually. The same procedures were used to dissolve iron (III) nitrate pentahydrate in 10 mL distilled water and mix it with 15 mL iso-butanol. The iron oxide nanoparticles were all rinsed in distilled water at 75°C before being dried in a 50°C oven. For 4 hours, dry iron oxide nanoparticles were calcined at 400°C [33]. Figure 1 shows the SEM image of iron oxide nanoparticles. To analyze the morphology and crystallite size, SEM analysis has been conducted. As confirmed by SEM micrograph.
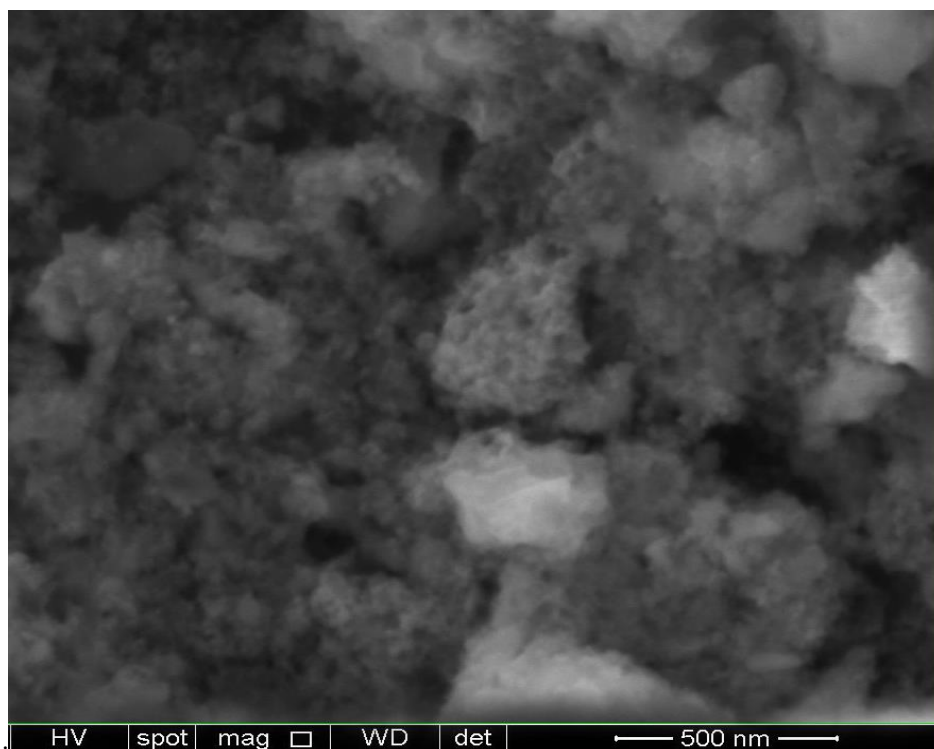

Fig. 1 Scanning electron microscopy (SEM) image of iron oxide nanoparticles

Apparatus and chemicals

A devoted exclusively to autos The electrochemical investigation was conducted using a potentiostat (Digi-ivy 2113 Texas, USA) with electrochemical system software for general use. In a mortar and pestle, we combined 0.7 grams of iron oxide nanoparticles with 1 gram of carbon powder and 0.5 milliliters of paraffin to form a homogeneous mixture. The end of the life cycle of a g. In order to keep the paste fresh, we needed to utilize a glass tube (diameter 0.4 mm length and 7 cm long). A platinum wire was inserted into the carbon paste to strengthen the electrical contact. Using a fine piece of paper, the carbon paste's surface was polished before use in the experiment. The preparation methods for the unmodified carbon paste electrode were the same as for the modified carbon paste electrode.

Discussion and Conclusion Manganese cyclic voltammetry research

Using cyclic voltammetry (CV) for oxidation and reduction in distal water with an iron oxide nanoparticle electrode at a scan rate of 0. 1 - 0.5 v. s^{-1}

_____

and a possible voltage range of 2 to -2 V, the electrochemical behavior of Fe_2Cl_3 was determined. Two oxidation peaks were definitely observed for Fe^{+2} and Fe^{+3} at scan rate 0.1 v. s^{-1}, for example. $E_{pox1}=-0.703$ V and $E_{pox2}=-1.010$ V were employed to obtain the anodic currents $I_{pox1}=1.7 \times 10^{-4}$ and $I_{pox2}=4.890 \times 10^{-4}$, respectively, which coincide with $E_{pox1}=-0.732$ V and $E_{pox2}=-1.040$ V. At $E_{pred}= -0.526$ V and $I_{pred}=-1.05 \times 10^{-4}$A, connectivity and a single reduction peak were both attained. There was no reaction in any of the other treatments, showing that the Fe_2O_3 NPs carbon paste electrode was an ion selective electrode for Fe

ion. The electrode response to iron ion was shown by the black curve. As you can see in Figure 2, the results vary depending on the scan rate.

because the process is diffusion rather than surface controlled, the reduction peaks were relocated to more negative potential values as rises accompanied by an increase in the current peak, where the value of E rang more than 59 mV for the oxidation and reduction peak refers to the Quist-reversible mechanism reaction in CV, and $Ip / v^{1/2}$ non-linear relationship means non-reversible process, and the value of E rang more than 59 mV for the oxidation and reduction peak.
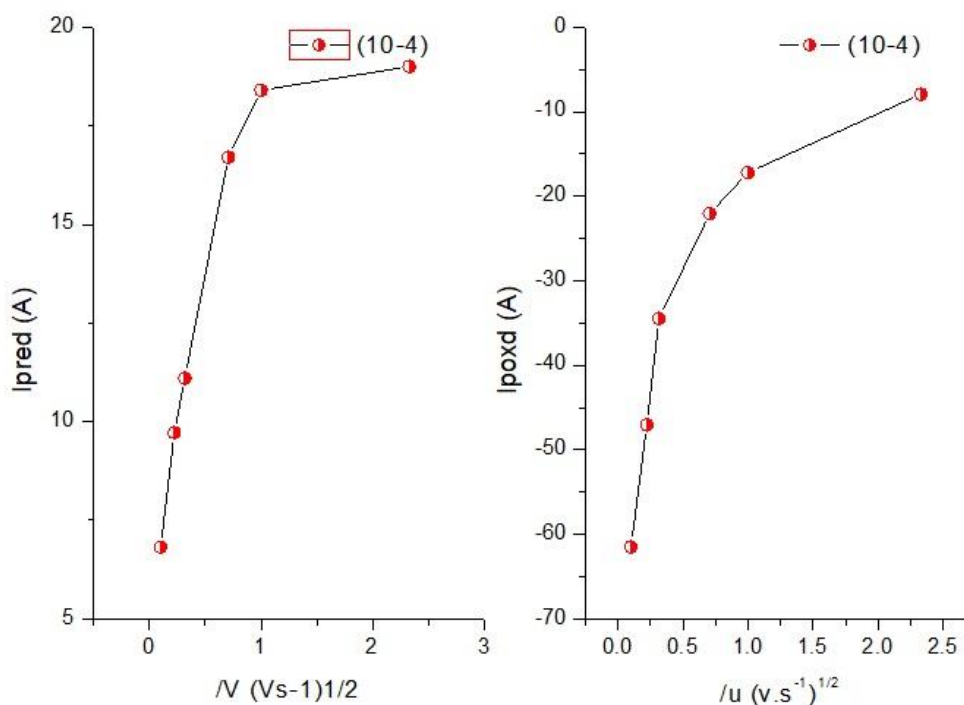

Figure 2: I_{pred1} and I_{pred2} peaks of reduction versus $\upsilon^{1/2}$ for Fe^{+2}.

Thermodynamic studies of the electro-oxidation of Fe_2O_3 NPs electrode.

From 15 to 35 degrees Celsius, CV investigated the electro-oxidation of electrodes. A cyclic voltammetry that can be reversed in a pinch. These parameters were obtained after observing that the curve had shifted upward and the slope had increased, indicating that reaction tacking was occurring on the electrode surface, where the temperature increased while the solvent temperature stayed constant [32, 34]. We found the scan rate rose, the beaks shifted to the negative side, indicating a clear signal using a carbon past electrode (working

electrode) covered with Fe3O4 nanoparticles. Figure 2 and table 1 illustrate the relationship between lnD to 1/T K, which is used to determine Ea (1). In addition to using Matsuda and Ayabe equations to calculate diffusion coffining, the researchers also used the equation = nF/RT to determine increased entropy when temperature was raised. These results pointed to a physical endothermic reaction when the values of -H and S indicated that entropy was rising as the temperature was raised. The rate constant response was calculated using the $K=k_o e^{-anf(E-E0)}$ equation. Moreover, a result of the electrode surface's first-order reaction was seen [35]. All of the data is presented in the following table (2).

Table (1) show the I-E data voltammograms for Fe_2O_3 NPs electrode Carbone past electrode with different temperature 15, 20, 25, 30 and 35 ℃, and diffusion coefficient for each step

TEMP. K	1/T 10^{-3}	E_{pa}	Ip_{oxd1} A (10^{-4})	E_{pa2}	Ip_{oxd2} A (10^{-4})	E_{pc}	Ip_{oxd} A (10^{-4})	$\Delta E = E_{pa}$ - E_{pc}	$\Delta E = E_{pa2}$ - $E_{pc}/2$	D. cof. Cm^2/s	Ln D
288	3.47	0.23	6.1	-0.57	8.40	1.3	12.1	-0.80	-1.0	2.1 - 10^{-9}	-25.1
293	3.41	0.23	6.1	-0.41	9. 42	1.1	8.8	- 0.64	- 0.9	2.8 - 10^{-9}	-24.9
298	3.33	0.29	5.2	-0.36	6.09	0.9	5.56	-0.65	-0.7	1.7 - 10^{-9}	-25.5
303	3.30	0.26	6.1	-0.48	6.73	1.1	10.10	- 0.74	- 1.0	1.6- 10^{-9}	-25.4
308	2.24	0.20	6.1	-0.55	5.62	1.2	9.10	-0.75	-1.0	1.1- 10^{-9}	-25.7

Table (2) Kinetic parameters of Fe_2O_3 NPs electrode Carbone past electrode

Type of electrode	ΔE KJ/mol	ΔH KJ/mol	ΔG KJ/mol	ΔS KJ/mol	K S^{-1} $10-5$	D^o x 10^{-7}	A	K_0
Fe2O3 NPs Carbone past electrode	-48.92	-5.79	-75.3	0.19	4.90	1.00	0.1	0.11

Fig. (3) effect of temperature on the cyclic voltammograms on Fe2O3 NPs electrode Carbone past electrode with different: 15, 20, 25, 30 and 35 ℃ respectably.

Calibration curve of iron at Fe2O3 NPs electrode Carbone past electrode

The analytical properties of the method were obtained by using the calibration graphs' linear ranges to establish the iron ion limits using a Carbone past electrode CV as the basis. interaction of iron ions with Fe_2O_3 nanoparticle electrode the cyclic voltammetry method and various concentrations of Fe_2Cl_3 pure stock solution were used to investigate the CPE. Figure (4) depicts the CV calibration curve in the (1–5) ppm range, as well as the application of the equation

w.t = (ppm M.wt Fe/M.wt sample)/ (10 V),

The molecular weight M.wt is the same as the substance's molecular weight, and volume V is the same as the substance's molecular weight. Using a dilution solution and a genuine sample of iron-containing vitamins, illustrate the findings.
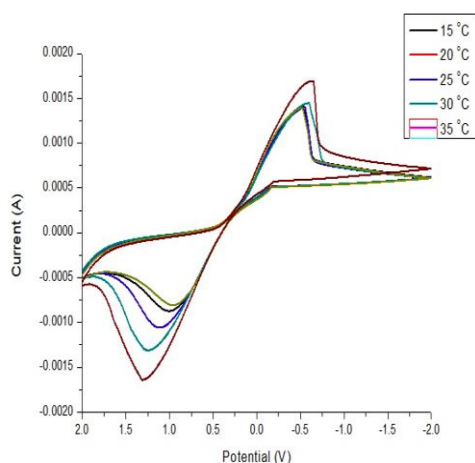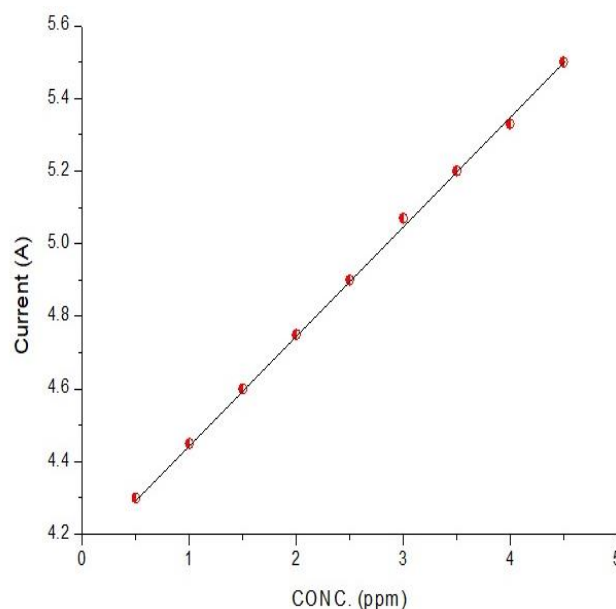
Fig. (4) Calibration curve by Fe_2O_3 NPs electrode Carbone past electrode for Fe_2Cl_3 solutions.

Table (2) show the result determined of real sample of drug by deferent method

Method	Analyte	Linear range	Founded	RSD %
Cyclic voltammetry		$10^{-3} – 10^{+3}$ ppm		
	Fe 2 mg		1.22 ppm	61.0%
	Fe 4 mg		3.09 ppm	77.2%
	Fe 6 mg		4.87 ppm	81.1%
Coulometry		$0.08 – 10^{+3}$ ppm		
	Fe 2 mg		1.21 ppm	60.5%
	Fe 4 mg		2.90 ppm	72.5%
	Fe 6 mg		5.19 ppm	86.5%
Atomic radiation		$0.1 - 10^{+3}$ ppm		
	Fe 2 mg		1.73 ppm	86.5%
	Fe 4 mg		3.62 ppm	90.5%
	Fe 6 mg		5.40 ppm	90.0%

Table (3) show the result determined of stock solution by deferent method

Cyclic voltammetry		$10^{-3} – 10^{+3}$ ppm		
	Fe 2 mg		1.51 ppm	75.5%
	Fe 4 mg		3.40 ppm	85.0%
	Fe 6 mg		5.0 ppm	83.3%
Coulometry		$0.01 – 10^{+3}$ ppm		
	Fe 2 mg		1.81 ppm	90.5%
	Fe 4 mg		2.87 ppm	71.7%
	Fe 6 mg		5.20 ppm	86.6%
Atomic radiation		$0.001 - 10^{+3}$ ppm		
	Fe 2 mg		1.97 ppm	98.5%
	Fe 4 mg		3.88 ppm	97.0%
	Fe 6 mg		5.39 ppm	89.8%

Conclusions

When Fe_2O_3 NPs are placed on top of an electrode, they are extremely sensitive and selective, detecting even minor changes in the current flowing through their solution. Compared to standard methods like the atomic analyser and colorimetric method in a real sample, the results were extremely accurate when it was used to make the electrodes before testing tiny amounts of iron-containing medicines in conventional solutions and investigate their physical and chemical properties

References

[1] V. Biju, Chemical modifications and bioconjugate reactions of nanomaterials for sensing, imaging, drug delivery and therapy, Chemical Society Reviews 43(3) (2014) 744-764.

[2] J.M. Campelo, D. Luna, R. Luque, J.M. Marinas, A.A. Romero, Sustainable preparation of supported metal nanoparticles and their applications in catalysis, ChemSusChem: Chemistry & Sustainability Energy & Materials 2(1) (2009) 18-45.

[3] D. Rathod, C. Dickinson, D. Egan, E. Dempsey, Platinum nanoparticle decoration of carbon materials with applications in non-enzymatic glucose sensing, Sensors and Actuators B: Chemical 143(2) (2010) 547-554.

[4] F.C. Vicentini, B.C. Janegitz, C.M. Brett, O. Fatibello-Filho, Tyrosinase biosensor based on a glassy carbon electrode modified with multi-walled carbon nanotubes and 1-butyl-3-methylimidazolium chloride within a dihexadecylphosphate film, Sensors and Actuators B: Chemical 188 (2013) 1101-1108.

[5] K. Tschulik, C. Batchelor-McAuley, H.-S. Toh, E.J. Stuart, R.G. Compton, Electrochemical studies of silver nanoparticles: a guide for experimentalists and a perspective, Physical Chemistry Chemical Physics 16(2) (2014) 616-623.

[6] R.C. Carvalho, A. Mandil, K.P. Prathish, A. Amine, C.M. Brett, Carbon nanotube, carbon black and copper nanoparticle modified screen printed electrodes for amino acid determination, Electroanalysis 25(4) (2013) 903-913.

[7] R. Liu, J. Duay, S.B. Lee, Redox exchange induced MnO2 nanoparticle enrichment in poly (3, 4-ethylenedioxythiophene) nanowires for electrochemical energy storage, Acs Nano 4(7) (2010) 4299-4307.

[8] M. Roushani, Z. Abdi, A. Daneshfar, A. Salimi, Hydrogen peroxide sensor based on riboflavin immobilized at the nickel oxide nanoparticle-modified glassy carbon electrode, Journal of Applied Electrochemistry 43(12) (2013) 1175-1183.

[9] D.-W. Kim, K.-Y. Rhee, S.-J. Park, Synthesis of activated carbon nanotube/copper oxide composites and their electrochemical performance, Journal of alloys and compounds 530 (2012) 6-10.

[10] X.Y. Kong, Y. Ding, R. Yang, Z.L. Wang, Single-crystal nanorings formed by epitaxial self-coiling of polar nanobelts, Science 303(5662) (2004) 1348-1351.

[11] X. Shen, Q. Zheng, J.-K. Kim, Rational design of two-dimensional nanofillers for polymer nanocomposites toward multifunctional applications, Progress in Materials Science 115 (2021) 100708.

[12] G.J. Long, Industrial applications of the Mössbauer effect, Springer Science & Business Media2012.

[13] A.B. Pai, 6. IRON OXIDE NANOPARTICLE FORMULATIONS FOR SUPPLEMENTATION, Essential Metals in Medicine: Therapeutic Use and Toxicity of Metal Ions in the Clinic (2019) 157-180.

[14] M. Magro, D. Baratella, E. Bonaiuto, J. de A Roger, F. Vianello, New perspectives on biomedical applications of iron oxide nanoparticles, Current medicinal chemistry 25(4) (2018) 540-555.

[15] E.A. Campos, D.V.B.S. Pinto, J.I.S.d. Oliveira, E.d.C. Mattos, R.d.C.L. Dutra, Synthesis, characterization and applications of iron oxide nanoparticles-a short review, Journal of Aerospace Technology and Management 7 (2015) 267-276.

[16] A. Bouafia, S.E. Laouini, Plant-mediated synthesis of iron oxide nanoparticles and evaluation of the antimicrobial activity: a review, Mini-Reviews in Organic Chemistry 18(6) (2021) 725-734.

[17] A. Tufani, A. Qureshi, J.H. Niazi, Iron oxide nanoparticles based magnetic luminescent quantum dots (MQDs) synthesis and biomedical/biological applications: A review, Materials Science and Engineering: C 118 (2021) 111545.

[18] M. Salehipour, S. Rezaei, J. Mosafer, Z. Pakdin-Parizi, A. Motaharian, M. Mogharabi-Manzari, Recent advances in polymer-coated iron oxide nanoparticles as magnetic resonance imaging contrast agents, Journal of Nanoparticle Research 23(2) (2021) 1-35.

[19] M. Firoz, M. Graber, Bioavailability of US commercial magnesium preparations, Magnesium research 14(4) (2001) 257-262.

[20] Y.-k. Sun, M. Ma, Y. Zhang, N. Gu, Synthesis of nanometer-size maghemite particles from magnetite, Colloids and Surfaces A: Physicochemical and Engineering Aspects 245(1-3) (2004) 15-19.

[21] K. Petcharoen, A. Sirivat, Synthesis and characterization of magnetite nanoparticles via the chemical co-precipitation method, Materials Science and Engineering: B 177(5) (2012) 421-427.

[22] A. Bee, R. Massart, S. Neveu, Synthesis of very fine maghemite particles, Journal of Magnetism and Magnetic Materials 149(1-2) (1995) 6-9.

[23] A. Jafari, S.F. Shayesteh, M. Salouti, K. Boustani, Effect of annealing temperature on magnetic phase transition in Fe3O4 nanoparticles, Journal of Magnetism and Magnetic Materials 379 (2015) 305-312.

[24] K. Rane, V. Verenkar, Synthesis of ferrite grade γ-Fe 2 O 3, Bulletin of Materials Science 24(1) (2001) 39-45.

[25] A.B. Chin, I.I. Yaacob, Synthesis and characterization of magnetic iron oxide nanoparticles via w/o microemulsion and Massart's procedure, Journal of materials processing technology 191(1-3) (2007) 235-237.

[26] K. Woo, H.J. Lee, J.P. Ahn, Y.S. Park, Sol–gel mediated synthesis of Fe2O3 nanorods, Advanced Materials 15(20) (2003) 1761-1764.

[27] E. Herrero, M. Cabanas, M. Vallet-Regi, J. Martinez, J. Gonzalez-Calbet, Influence of synthesis conditions on the γ-Fe2O3 properties, Solid State Ionics 101 (1997) 213-219.

[28] M.P. Reddy, A. Mohamed, X. Zhou, S. Du, Q. Huang, A facile hydrothermal synthesis, characterization and magnetic properties of mesoporous CoFe2O4 nanospheres, Journal of Magnetism and Magnetic Materials 388 (2015) 40-44.

[29] K. Woo, J. Hong, S. Choi, H.-W. Lee, J.-P. Ahn, C.S. Kim, S.W. Lee, Easy synthesis and magnetic properties of iron oxide nanoparticles, Chemistry of materials 16(14) (2004) 2814-2818.

[30] T. Raming, A.J. Winnubst, C.M. van Kats, A. Philipse, The synthesis and magnetic properties of nanosized hematite (α-Fe2O3) particles, Journal of Colloid and Interface Science 249(2) (2002) 346-350.

[31] O. Karaagac, H. Kockar, A simple way to obtain high saturation magnetization for superparamagnetic iron oxide nanoparticles synthesized in air atmosphere: Optimization by

experimental design, Journal of Magnetism and Magnetic Materials 409 (2016) 116-123.

[32] D. Kostyukova, Y.H. Chung, Synthesis of iron oxide nanoparticles using isobutanol, Journal of Nanomaterials 2016 (2016).

[33] S. Gupta, M. Tripathi, A review on the synthesis of TiO2 nanoparticles by solution route, Open Chemistry 10(2) (2012) 279-294.

[34] E.S. Abood, A.M. Jouda, M.S. Mashkoor, Zinc metal at a new ZnO nanoparticle modified carbon paste electrode: a cyclic voltammetric study, Nano Biomed Eng 10(2) (2018) 149-155.

[35] E.S. Abood, M.S. Mashkoor, A.M. Jouda, Cyclic Voltammetry Study for MnO2 Nanoparticles Modified Carbon Paste Electrode, Nano Biomed. Eng 11(4) (2019) 368-374.